

# Optical coherence and Doppler tomography for monitoring tissue changes induced by laser thermal therapy—An *in vivo* feasibility study

Victor X. D. Yang, Julius Pekar, Stewart S. W. Lo, Maggie L. Gordon, Brian C. Wilson, and I. Alex Vitkin<sup>a)</sup>

*Departments of Medical Biophysics and Radiation Oncology, University of Toronto, Toronto, Ontario M5G 2M9, Canada and Division of Medical Physics, Ontario Cancer Institute/University Health Network, and Biophotonics Facility, Photonics Research Ontario, Toronto, ON M5G 2M9, Canada*

(Presented on 24 June 2002)

A high-speed optical coherence and Doppler tomography system suitable for real-time monitoring of the microstructural and microvascular tissue changes induced by laser thermal therapy is described. The performance of the system is demonstrated experimentally *in vivo* by noting the morphological change, manifest as an increase in the optical extinction coefficient, and the reduction in the blood flow during and after laser thermal therapy in an animal model. © 2003 American Institute of Physics. [DOI: 10.1063/1.1519680]

## I. INTRODUCTION

Optical coherence tomography (OCT)<sup>1</sup> and its Doppler<sup>2,3</sup> extension are relatively new imaging techniques developed for noninvasive biomedical applications. OCT detects back-scattered photons from subsurface microstructures up to 2 mm deep in tissue, and performs depth discrimination by low-coherence interferometry with the resolution ranging from 2 to 15  $\mu\text{m}$ .<sup>4,5</sup> Similar in principle to Doppler ultrasound, Doppler OCT, or optical Doppler tomography (ODT) can detect moving particles using the Doppler effect, which is useful in measuring blood flow in tissue. Because the optical wavelength is one to two orders of magnitude smaller than the acoustic wavelength, ODT can detect much slower blood flow velocity ( $\sim 0.05$  mm/s) than Doppler ultrasound, and is thus capable of imaging capillary flow *in vivo*. Previously, we developed a digital signal processing technique for ODT that can measure blood flow velocities over a large range ( $-7$  to  $+7$  mm/s at  $75^\circ$  Doppler angle) and reject tissue motion artifacts.<sup>6</sup> In this article, we present the feasibility study of using our OCT/ODT system to monitor the microstructural and microvascular changes induced by laser thermal therapy in an animal model.

## II. APPARATUS

A schematic of the OCT/ODT system is shown in Fig. 1. Its detailed operation has been described previously.<sup>6</sup> Briefly, a continuous-wave broadband infrared source emits approximately 5 mW centered at 1300 nm wavelength with 62 nm bandwidth. The emission is passed through a Michelson fiber interferometer, which produces an interference pattern with a coherence length of  $\sim 14$   $\mu\text{m}$  in air. This corresponds to an axial spatial resolution (in the  $z$  direction) of 10  $\mu\text{m}$  in biological tissue (assuming a refractive index of 1.4). Lateral spatial resolution is determined by the spot size of the light beam incident on the sample, which is about 10  $\mu\text{m}$  at the

focal point with a confocal parameter of about 400  $\mu\text{m}$ . Three-dimensional (3D) imaging is accomplished by two motorized translation stages for  $x$ - and  $y$ -axes scanning in the sample arm, and by a rapid scanning optical delay (RSOD) line for  $z$ -axis ranging in the reference arm. The field of view of an  $x$ - $z$  image is 3.60 mm $\times$ 0.62 mm, and the  $y$ -axis increment between the adjacent image slices is 10  $\mu\text{m}$ . The amplitude of the interference pattern corresponds to the depth-resolved reflectivity in the sample, and its logarithm is displayed as a structural image, analogous to  $B$ -mode ultrasound display. The phase difference between consecutive  $z$ -axis scans is related to the Doppler frequency shift caused by moving particles, such as red blood cells. The Doppler shift is color coded to form a blood flow image analogous to color-Doppler ultrasound. Unlike ultrasound, which requires a coupling agent such as gel or water-bath, OCT/ODT imaging is noncontact. Both the structural and flow images (in the  $x$ - $z$  plane) are digitized into 600( $x$ ) $\times$ 312( $z$ ) pixels which are acquired, processed, and displayed at imaging speed of one frame per second. The image quality can be improved by averaging multiple subsequent  $z$ -axis scans, to increase the signal-to-noise ratio in the structural image and the velocity sensitivity in the color flow image, albeit at the expense of a reduced frame rate.

## III. ANIMAL FEASIBILITY EXPERIMENT

Malignant human melanoma cells (ATCC HTB-67) were implanted intradermally into the hind leg skin of severe combined immunodeficiency (SCID) mice, which resulted in solid tumors of 5–7 mm in diameter after  $\sim 6$  weeks. Prior to OCT/ODT imaging, the animal was anesthetized and placed into a mouse restrainer as shown in Fig. 2(A). The hind legs were shaved and secured with surgical tape. The tumors were irradiated with 760 nm light at 3 W/cm<sup>2</sup> for 3 min, with a spot size of 7 mm diam. OCT/ODT imaging was performed immediately before, immediately after, and at 3, 6, and 24 h post laser treatment. Interrogating a total volume of 3.6  $\times$  0.6  $\times$  0.4 mm<sup>3</sup>, 40 slices of OCT/ODT images were taken

<sup>a)</sup> Author to whom correspondence should be addressed; electronic mail: vitkin@uhnres.utoronto.ca

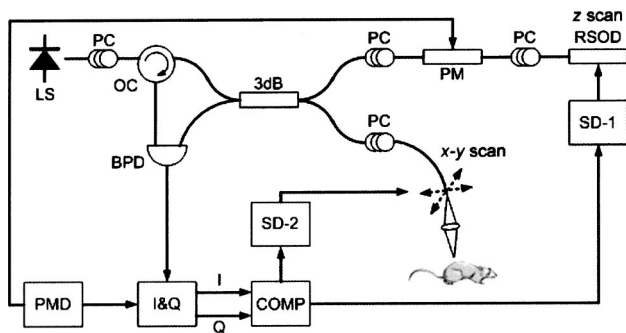


FIG. 1. Schematic of the OCT/ODT system: LS, light source; PC, polarization controller; OC, optical circulator; 3dB, fiber optic coupler; PM, phase modulator; RSOD, rapid scanning optical delay for  $z$  axis scan; SD-1 and 2, scan drivers for  $x$  and  $y$  axes; PMD, phase modulator driver; BPD, balanced photodetector; I and Q, in-phase and quadrature demodulator; and COMP, computer (see Ref. 6 for more details).

at each time point. Although small positioning error could occur for the 3, 6, and 24 h post-treatment scans, attempts were made to image the same volume. The tumor was resected and stained with heamatoxylin and eosin 24 h after treatment, for subsequent histological evaluation and OCT/ODT comparison.

#### IV. RESULTS

Preliminary results show that tissue changes induced by laser thermal therapy can be detected by OCT/ODT without motion artifacts. One of the 40 OCT images obtained before laser therapy is shown in Fig. 2(B), illustrating the microstructure of the implanted tumor and the overlying skin. Although not clearly visible in the structural image, three blood vessels of diameters ranging from 10 to 20  $\mu\text{m}$  are visible in the ODT image, as shown in Fig. 2(C). The Doppler frequency shifts present in these vessels range from about  $-600$  Hz (flowing away from the skin surface) to  $+2$  kHz (flowing towards the skin surface). The actual blood flow velocity,  $V$ , can be calculated from

$$V = \frac{\lambda_0}{2n \cos(\theta)} f_D,$$

where  $\lambda_0$  is the central light wavelength,  $f_D$  is the Doppler frequency shift (obtained from the measured phase shift),  $n$  is the average refractive index of tissue ( $\sim 1.4$ ), and  $\theta$  is the

Doppler angle between the direction of blood flow and the incident light. The Doppler angle can be estimated by comparing the position of the blood vessel across multiple ODT images taken at different  $y$ -axis positions. However, since capillaries (diameter  $\sim 10$ – $20$   $\mu\text{m}$ ) are quite tortuous, we assumed a Doppler angle of  $75^\circ$  for all blood vessels in this feasibility study. This assumption gives a measured blood flow velocity range of  $-1.0$  to  $+3.6$  mm/s in these blood vessels. Another measure of blood perfusion is the amount of moving blood in the imaged volume. This is obtained by calculating the area occupied by blood vessels in each image, and accumulated across all images in the volume. For the tumor shown in Fig. 2, the moving blood occupies approximately 0.2% of the total tissue volume imaged.

Figure 3 shows the OCT and ODT images of the tumor immediately after the 3 min laser irradiation and at 3, 6, and 24 h post-treatment. As shown in Fig. 3(A), it is clear that the layered morphology of the overlying skin above the tumor became much less visible immediately after treatment, as compared with Fig. 2(B). Apart from the morphological change, the penetration depth of the OCT imaging was greatly reduced. This can be quantified by fitting the logarithm of the interference amplitude as a function of the depth into tissue, which is approximately the optical attenuation coefficient of the tissue at 1300 nm. For this calculation, 50 axial scans of the OCT signal profiles were averaged along the  $x$  direction, normalized to the maximum of each profile, and the results are shown in Fig. 4. The linear fit was carried out using only the first half of the signal profile (where the normalized OCT signal  $> 0.5$ ), since at deeper depths single backscattering events no longer dominate, and the attenuation is no longer described by the simple decaying exponential.<sup>7</sup> The calculated tissue optical attenuation coefficient for the pretreatment time point is  $80 \pm 15$   $\text{cm}^{-1}$  (SD), significantly different from that of the immediately post-treatment time point, which is  $200 \pm 10$   $\text{cm}^{-1}$ . The smaller error in the post-treatment case is indicative of the less structured, more homogeneous tissue morphology resulting from the laser irradiation, as seen in comparing the structural OCT images of Fig. 3 with that of Fig. 2(B). At 3 h post-treatment, the animal was reanesthetized and imaged again; in this case, the calculated tissue optical extinction coefficient was  $150 \pm 10$   $\text{cm}^{-1}$ . This trend of reduced penetration of OCT signal

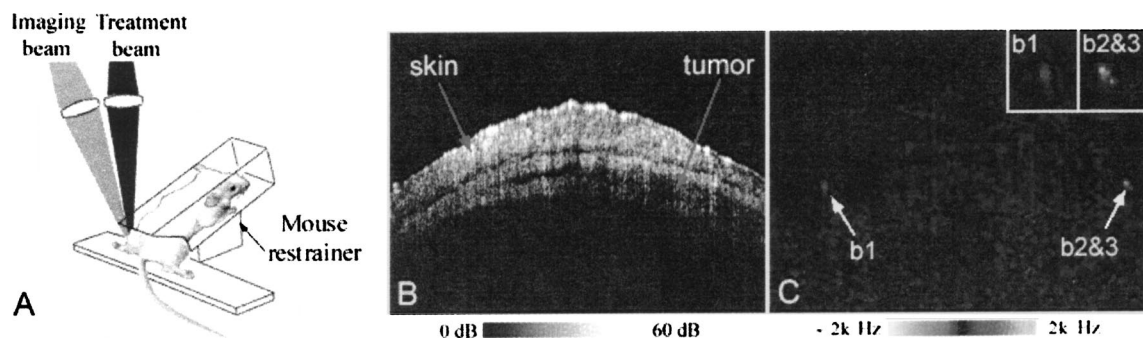


FIG. 2. (A) Animal experiment setup with the mouse restrainer. (B) Typical OCT structural image of the mouse hind leg region with the implanted melanoma and overlying skin (notice the layered morphology). (C) Corresponding ODT color flow image of the same region, where three small blood vessels (b1, b2, b3) situated between the tumor and skin can be found. Inset: zoom-in view ( $\times 2$ ) of the three blood vessels. This set of images was obtained prior to laser thermal therapy. Image dimension: 3.6 mm ( $x$ ) lateral  $\times$  0.6 mm ( $z$ ) depth.

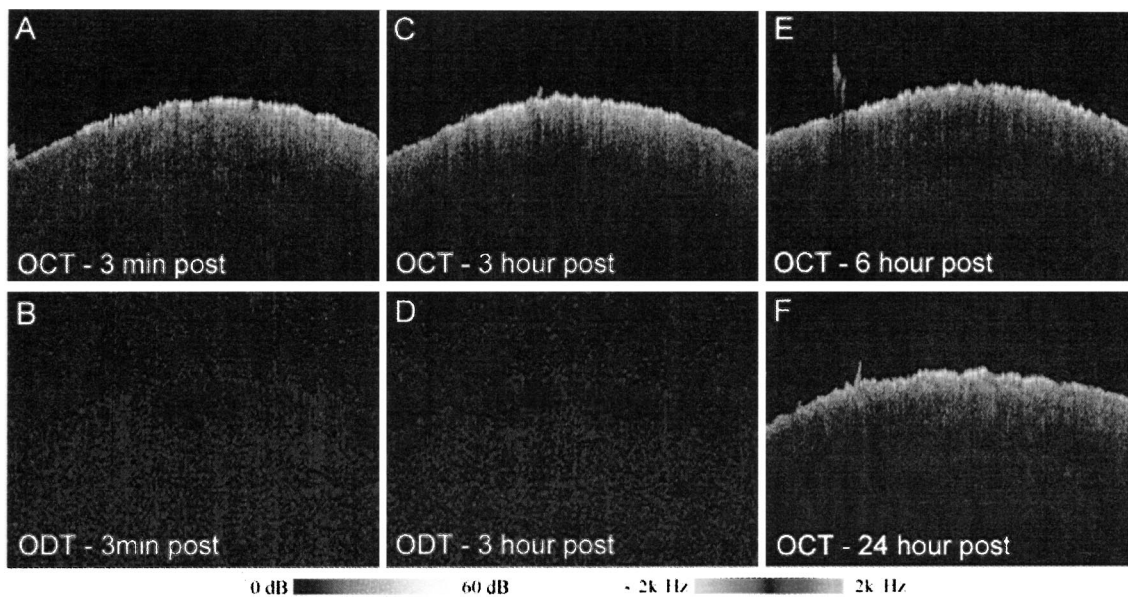


FIG. 3. OCT/ODT images obtained at various time points postlaser thermal therapy. Immediately post-therapy (3 min after onset of treatment laser), the treated region showed reduction in the OCT signal, as displayed in (A). Corresponding ODT image in (B) showed no sign of blood vessels, indicating complete vascular shutdown. Similar results were obtained at the 3 h time point, as shown in (C) and (D). The reduction in OCT signal was persistent, as shown in (E) at the 6 h and (F) at the 24 h time point. The Doppler images for the 6 and 24 h time points are not shown here; similar to the earlier post-treatment scans, no blood vessels were found. Image dimension: 3.6 mm width  $\times$  0.6 mm depth.

was also observed at the 6 and 24 h post-treatment time points.

Accompanying the changes in morphology and optical extinction, blood flow in the treated region was significantly reduced. Figures 3(B) and 3(D) show the corresponding Doppler flow images immediately post-laser thermal therapy, and at 3 h after. No blood vessels were found in these images for the entire scanned volume when all image slices were analyzed.

## V. DISCUSSIONS

Real-time monitoring of the tissue changes is important for laser thermal therapy for two reasons: (1) to ensure treat-

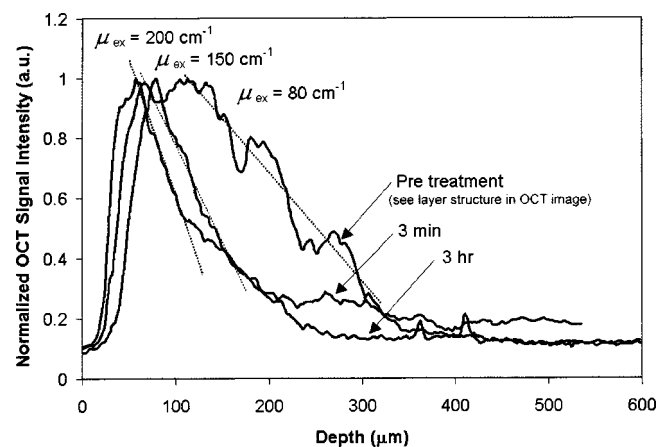


FIG. 4. Normalized average OCT signal (logarithm of the backscattering photon interference fringe intensity) as a function of depth into tissue. Solid lines indicate the OCT signal at three time points (pretreatment, 3 min post-treatment, and 3 h post-treatment). Dashed lines are linear fits to the signal, indicating the resulting average optical attenuation coefficients. The peaks and valleys of the pretreatment curve correspond to the structured layer morphology seen in the OCT image of Fig. 2(A); these are reduced following laser treatment (OCT images of Fig. 3).

ment is adequate; and (2) to prevent damage to surrounding normal tissue. Imaging methods like ultrasonography, computed tomography (CT), and magnetic resonance imaging (MRI) have been attempted but have limitations.<sup>8</sup> The main difficulty with ultrasound monitoring is the uncertainty of whether the observed changes are reversible or irreversible. CT and MRI cannot presently monitor tissue changes in real time and are expensive. On the other hand, all three type of changes (morphological, optical extinction, and blood flow) observed with OCT/ODT in our feasibility study seemed to be irreversible (additional imagings were conducted at 6 and 24 h post-treatment, with similar trends). The change in the tissue optical extinction coefficients induced by the laser thermal therapy is likely due to an increase in the scattering coefficient,<sup>9</sup> as at 1300 nm the optical attenuation is dominated by scattering instead of absorption. Our preliminary results are similar to previous OCT experiments on thermally damaged skin tissue.<sup>10</sup> It is possible to obtain even higher contrast between laser-treated and untreated tissue by employing polarization-sensitive OCT in certain tissues, especially those with birefringence such as the skin.<sup>11</sup>

Laser thermal therapy induced changes in perfusion have been reported previously using Doppler ultrasound<sup>12</sup> and two-dimensional ODT.<sup>13</sup> In comparison with ultrasound, the advantage of our OCT/ODT method is the improved spatial and velocity resolution, thus allowing the detection of vascular shutdown in blood vessels 10–100 times smaller. The main disadvantage is the reduced imaging depth, which could be overcome by using interstitial OCT/ODT probes. In fact, such interstitial OCT/ODT probes may also be used as fluence probes for real-time monitoring and feedback control of the laser thermal therapy. Further investigations with a larger number of animals, a variety of irradiation conditions, and optothermal denaturation models are required to extend

this feasibility study to evaluate the potential of OCT/ODT as a quantitative monitoring tool for laser thermal therapy.

## ACKNOWLEDGMENTS

The authors acknowledge the experimental assistance provided by Anoja Giles, Mark Jarvi, Lee Chin, and Dr. Mike Kolios, Dr. Greg Czarnota, and Dr. Robert Weersink. The OCT/ODT development is funded by the Natural Science and Engineering Council of Canada, Canadian Institutes of Health Research, Photonics Research Ontario, Ontario Cancer Institute, and St. Michael's Hospital in Toronto.

<sup>1</sup>D. Huang, E. A. Swanson, C. P. Lin, J. S. Schuman, W. G. Stinson, W. Chang, M. R. Hee, T. Flotte, K. Gregory, C. A. Puliafito, and J. G. Fujimoto, *Science* **254**, 1178 (1991).

<sup>2</sup>Z. Chen, T. E. Milner, D. Dave, and J. S. Nelson, *Opt. Lett.* **22**, 64 (1997).

<sup>3</sup>S. Yazdanfar, M. D. Kulkarni, and J. A. Izatt, *Opt. Express* **1**, 424 (1997).

<sup>4</sup>J. A. Izatt, M. D. Kulkarni, H. Wang, K. Kobayashi, and M. V. Sivak, *IEEE J. Sel. Top. Quantum Electron.* **2**, 1017 (1996).

<sup>5</sup>W. Drexler, U. Morgner, F. X. Kartner, C. Pitris, S. A. Boppart, X. D. Li, E. P. Ippen, and J. G. Fujimoto, *Opt. Lett.* **24**, 1221 (1999).

<sup>6</sup>V. X. D. Yang, M. L. Gordon, A. Mok, Y. Zhao, Z. Chen, R. S. C. Cobbold, B. C. Wilson, and I. A. Vitkin, *Opt. Commun.* **208**, 209 (2002).

<sup>7</sup>J. M. Schmitt, A. Knüttel, M. Yablowsky, and M. A. Eckhaus, *Phys. Med. Biol.* **39**, 1705 (1993).

<sup>8</sup>F. A. Jolesz, in *Laser-Induced Interstitial Thermotherapy*, 1st ed., edited by G. Muller (SPIE, Bellingham, 1995), Chap. V, p. 265.

<sup>9</sup>L. Chin, W. M. Whelan, M. D. Sherar, and I. A. Vitkin, *Phys. Med. Biol.* **46**, 2407 (2001).

<sup>10</sup>J. F. de Boer, S. M. Srinvas, A. Malekafzali, Z. Chen, and J. N. Nelson, *Opt. Express* **3**, 212 (1998).

<sup>11</sup>K. Schoenenberger, B. W. Colston, D. J. Maitland, L. B. Da Silva, and M. J. Everett, *Appl. Opt.* **37**, 6026 (1998).

<sup>12</sup>E. Rohde, C. Philipp, and H. Berlien, in *Laser-Induced Interstitial Thermotherapy*, 1st ed., edited by G. Muller (SPIE, Bellingham, 1995), Chap. V, p. 267.

<sup>13</sup>J. N. Barton, A. J. Welch, and J. A. Izatt, *Opt. Express* **3**, 251 (1998).